DOI: 10.1002/chem.200800610

Novel Cyclic Sulfonium-Based Ionic Liquids: Synthesis, Characterization, and Physicochemical Properties

Qinghua Zhang,[a, b, c] Shimin Liu,[a] Zuopeng Li,[a] Jian Li,[a] Zhengjian Chen,[a] Ruifeng Wang,[a] Liujin Lu,[a] and Youquan Deng*[a]

Abstract: A new series of ionic liquids composed of three cyclic sulfonium cations and four anions has been synthesized and characterized. Their physicochemical properties, including their spectroscopic characteristics, ion cluster behavior, surface properties, phase transitions, thermal stability, density, viscosity, refractive index, tribological properties, ion conductivity, and electrochemical window have been comprehensively studied. Eight of these salts are liquids at room temperature, at which some salts based on $[NO_3]^-$ and $[NTf_2]^-$ ions exhibit organic plastic crystal behaviors, and all the saccharin-based salts display relatively high refractive indices (1.442–1.594). In addition, some ionic liquids with the $[NTf_2]^-$ ion exhibit peculiar spectroscopic characteristics in FTIR and UV/Vis regions, whilst those salts based on the $[DCA]^-$ ion show lower viscosities (34.2–62.6 mPa s at 20 °C) and much higher conductivities (7.6–17.6 mS cm^{-1} at 20 °C) than most traditional 1,3-dialkylimidazolium salts.

Keywords: electrochemistry · ionic liquids · performance · physicochemical properties · sulfonium ions

Introduction

Over the past decade, the interest in ionic liquids (ILs) has been increasing with surprising speed, mainly stimulated by the appearance of numerous new ILs with peculiar properties[1–3] and ever-increasing applications in both academia and industry in fields as diverse as electrochemistry,[4] synthesis,[5] catalysis,[6] materials,[7] separation,[8] and biotechnology.[9] Although there are, in theory, potentially millions of ILs available through the combination of different cations and anions, up to now only thousands of ILs have been developed and used, most of which are based on imidazolium,[10] pyrrolidinium,[11] tetraalkylammonium,[12] pyridinium,[13] and quaternary phosphonium[14] ions. Thus, one of the hot topics in the field of IL research is the molecular design and synthesis of novel ILs, in particular ILs with peculiar physicochemical characteristics and special applications. After a period of prosperity in which conventional ILs were predominantly used as environmentally benign media in synthesis and catalysis, interest in ILs by the scientific community has recently begun to revert to the field of electrochemistry,[15] for which these innovative liquids were initially developed. One key area of current research is the development of IL-based electrolytes for lithium ion batteries,[16] fuel cells,[17] capacitors,[18] solar cells,[19] and other electrochemical devices.

The emergence of functionalized ILs has endowed them with huge diversity both in quantity and properties, and has left more scope for further development.[20] Unfortunately, for ILs with NH_2,[21] SH,[22] OH,[23] COOH,[24] CN,[25] or $NHCONH_2$[26] as functional groups attached, a salient problem blocking their further applications is the relatively higher viscosity than organic solvents and the lower conductivity resulting from the high viscosity. From an electrochemical point of view, an ideal ionic liquid should possess the following desirable properties: 1) low melting point, <25 °C; 2) high ion conductivity; 3) good electrochemical stability; and 4) relatively low viscosity. To achieve the above targets, more effort should be dedicated to the devel-

[a] Dr. Q. Zhang, S. Liu, Z. Li, J. Li, Z. Chen, R. Wang, L. Lu, Prof. Y. Deng
Centre for Green Chemistry and Catalysis
Lanzhou Institute of Chemical Physics
Chinese Academy of Sciences
Lanzhou, 730000 (China)
Fax: (+86) 931-496-8116
E-mail: ydeng@lzb.ac.cn

[b] Dr. Q. Zhang
Graduate School of the Chinese Academy of Sciences
Beijing, 100039, PRC (China)

[c] Dr. Q. Zhang
School of Information Science and Engineering and
The National Laboratory of Applied Organic Chemistry
Lanzhou University, Lanzhou, 73000 (China)

opment of new ILs with the characteristics of ideal electrolytes.[27,28] Recently, a new family of ILs based on symmetrical and asymmetric trialkylsulfonium cations began to receive the interest of IL researchers, owing to the low viscosity and high conductivity of these systems.[29–32] For example, Wasserscheid et al. developed a series of ILs based on trialkylsulfonium dicyanamides, which were found to have low viscosity at extremely low temperature, for example, $\eta =$ 94.9 mPa s at −20 °C for triethylsulfonium dicyanamide.[33] Hydrophobic trialkylsulfonium ILs based on perfluorinated anions were also reported, and their potential applications as promising electrolytes in lithium batteries and dye-sensitized solar cells were preliminarily investigated.[34] However, information on the synthesis of ILs based on a cyclic sulfonium cation is relatively limited in previous literature.[35] Therefore, there is still some room to develop new sulfonium-based ILs that may be liquids at lower temperatures, and it should be expected that these novel ILs would possess the characteristics of low viscosity and high conductivity.

In this work, a new family of cyclic sulfonium-based ILs was systematically synthesized, and the detailed study of their physicochemical characteristics, including their spectroscopic properties, ion cluster behavior, surface properties, phase transitions, heat capacity, thermal stability, density, viscosity, refractive index, tribological properties, ion conductivity, and electrochemical stability, is particularly emphasized.

Results and Discussion

Synthesis and characterization: The structures and abbreviations of the cations and anions of twelve new ILs are shown in Scheme 1. All the cyclic sulfonium salts were prepared according to a similar approach reported previously.[33] Methylated tetrahydrothiophene iodide ([S1]I) was prepared with a high yield from the reaction of tetrahydrothiophene and the appropriate amount of iodomethane in acetone. Ethylated tetrahydrothiophene iodide ([S2]I) and butylated tetrahydrothiophene iodide ([S4]I) were prepared by using a similar reaction of tetrahydrothiophene with iodoethane or *n*-butyl iodide in acetone or anhydrous diethyl ether. The silver dicyanamide (AgDCA) was precipitated by mixing aqueous solutions of silver nitrate and sodium dicyanamide (1:1 molar ratio). The saccharin silver (AgSac) was also prepared by a similar method. The desired sulfonium salts with the target anion could be obtained easily and with high quality through an anion-exchange reaction between the above-mentioned three iodides (i.e., [S1]I, [S2]I, and [S4]I) with the corresponding inorganic salts (i.e., AgDCA, AgSac, and $LiNTf_2$) with a molar ratio of 1:1.1. All new cyclic sulfonium-based ILs were obtained with yields of 89–94%, and they are all stable to moisture. Among these ILs, [S1]DCA, [S2]DCA, [S4]DCA, [S4]NTf_2, [S1]Sac, [S2]Sac, [S4]Sac, and [S2]NO_3 are colorless liquids at room temperature and are miscible with water except for [S4]NTf_2; the others are white solids at room temperature. The structures and compositions of all ILs were confirmed by ^{1}H NMR and FTIR spectroscopy, and ESI mass spectrometry. The water content in the ILs was detected by a coulometric Karl-Fischer titration. The thermal properties of all the prepared salts were characterized by differential scanning calorimetry (DSC) and thermogravimetric analysis (TGA). For those salts that are liquid at room temperature, their densities (ρ), viscosities (η), refractive indices (n), friction coefficients (FC), ionic conductivities (κ), and electrochemical windows (EW) were measured. All the measured data are summarized in Tables 1–4. The effect of structural variations in the cation and anion on the above properties of these salts will be discussed below based on the results presented in these tables.

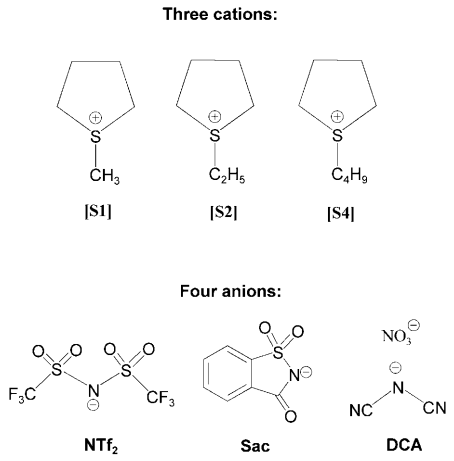

Scheme 1. Structures and abbreviations of the cations and anions employed in this work.

Product purity: Data on the purity of any new class of ILs are critical to the assessment of their physicochemical properties. Thus, the purity of the ILs was determined before each test of physicochemical properties. To ensure that the amount of water and other volatile solvents in the ILs was reduced as much as possible, each IL was kept in a vacuum (pressure 10^{-2}–10^{-3} mbar) at 90–100 °C for 2–4 h before every test. The purity of each IL was first verified by NMR spectroscopy to check for residues of unreacted reactants or residual solvents, and the analysis results indicated that these compounds had been completely eliminated. The water content in the ILs was determined by means of a Karl–Fischer titration (Mitsubishi CA-06 Moisturemeter). The water content in [S4]NTf_2 was 32 ppm (after drying at 100 °C for 2 h) owing to its hydrophobicity, whereas the hydrophilic $[DCA]^-$, $[NO_3]^-$, and $[Sac]^-$ salts still contained a water content of 200–400 ppm, even after rigorous drying at 90 °C and 10^{-2}–10^{-3} mbar for 4 h (see Table 2). It is worth noting that during the measurement of some properties (e.g., viscosity, conductivity, and refractive index) the ILs need to be exposed to the open ambient air, and the water in the air will inevitably pollute the ILs, especially those hydrophilic ILs. To find out how quickly these ILs absorb water from the ambient air, the hydrophilic ILs [S2]DCA

and [EMIm]BF_4 as well as the hydrophobic [S4]NTf_2 were exposed to the open ambient for 1, 5, and 30 min. The results showed that the rate of water absorption was relatively faster at the initial stages, and the rates for the hydrophilic [S2]DCA and [EMIm]BF_4 ILs were remarkably higher than that of the hydrophobic [S4]NTf_2 (Figure 1). For example, when the hydrophilic ILs [S2]DCA and [EMIm]BF_4 were exposed to the ambient for 5 min, approximately 70–80 ppm water was absorbed into the ILs, whereas under the same conditions the water content increased from 50 ppm to 80 ppm for hydrophobic [S4]NTf_2. Further prolonging the exposed time to 30 min, around 250–300 ppm water was absorbed into [EMIm]BF_4 and [S2]DCA, but just 120 ppm for hydrophobic [S4]NTf_2. This means that changes in water content in the ILs (particularly for the hydrophilic ILs) occurred during those measurements conducted under open ambient conditions (viscosity, conductivity, and refractive index). However, these measurements could be performed within 1–3 min, which means that although the slight increase in water content would certainly cause some measurement errors, such errors should be acceptable. The cyclic voltammetry analysis showed that no reducible or oxidizable species such as I^- and Ag^+ were detectable in the ILs, indicating that the metathesis reaction had been conducted completely and the purities of the ILs were all of electrochemical grade.

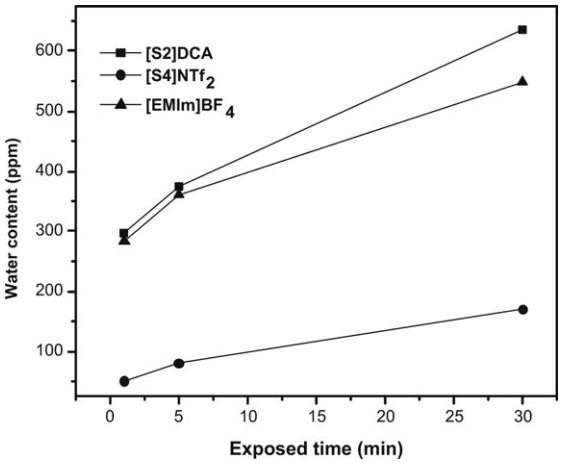

Figure 1. Water contents of four selected ILs at different exposure times.

NMR and FTIR spectra: ^{1}H NMR and FTIR spectroscopy were used to characterize the structures of the ILs prepared, and the information obtained showed that they are all the expected compounds (see Experimental Section). As shown by the ^{1}H NMR spectra of [S4]DCA in Figure 2, although the hydrogen atoms of C1–H and C4–H (or C2–H and C3–H) are chemically equivalent in the tetrahydrothiophene molecule, a chemical shift difference was clearly observed when an alkyl group was attached to the sulfur atom to form the sulfonium cation. The splitting of the signal related to these two kinds of CH_2 group (1,4–CH_2 and 2,3–CH_2) demonstrated that the introduction of the alkyl group had some influence on the steric location of the hydrogen atoms of the four CH_2 groups, resulting in an emerging difference in the chemical shifts. Moreover, the extent of peak splitting can be assigned to the electronic environment provided by the $[S]^+$ cation, that is, the splitting of the 1- and 4-position hydrogen atoms is more obvious than that of the 2- and 3-position hydrogen atoms because the former are attached directly to the $[S]^+$ ion.

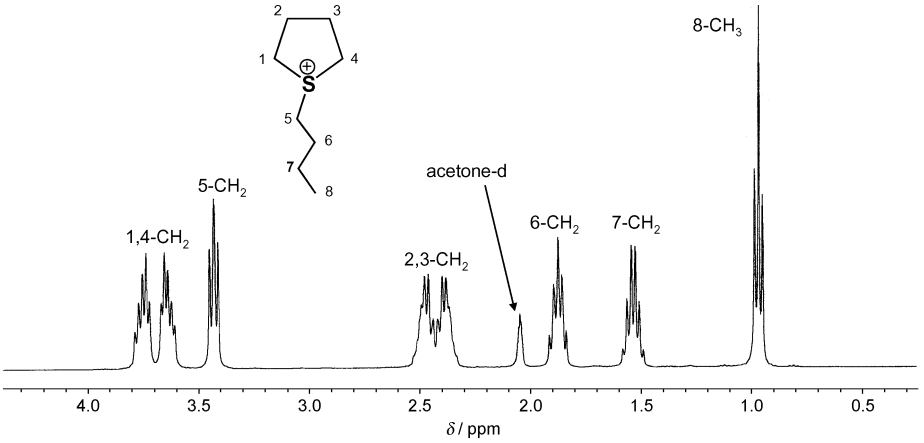

Figure 2. ^{1}H NMR spectrum of [S4]DCA.

For the FTIR spectra of all new ILs, the absorption frequencies of the aliphatic C–H vibrations in the cation ring or the alkyl group were mainly observed in the range of 2875–3021 cm^{-1}. Figure 3 gives the molecular vibration spec-

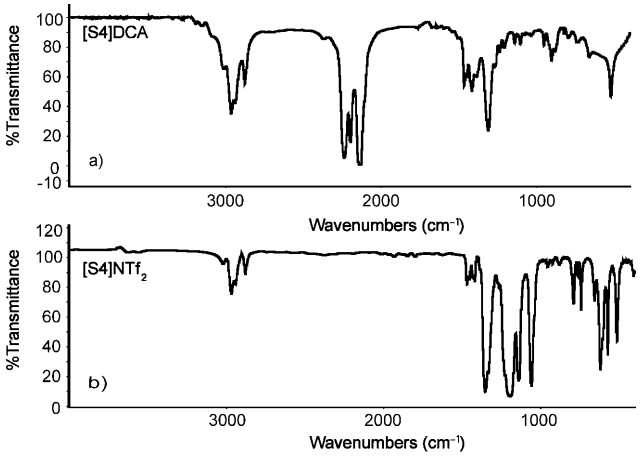

Figure 3. The FTIR spectra of a) [S4]DCA and b) [S4]NTf_2.

tra of [S4]DCA and [S4]NTf_2. From Figure 3b, we can see a good example of a C–H stretch of an aliphatic heterocyclic compound, where we observe the asymmetric C–H stretch of the methyl and methylene groups (2967 and 2940 cm^{-1}, respectively) occurring at slightly higher frequency than the symmetric vibration of the methyl group at 2879 cm^{-1}. Surprisingly, no strong absorptions in the range 1352–2880 cm^{-1} were observed in the FTIR spectrum of [S4]NTf_2 (Figure 3b). Thus, this salt might be a potential IR-transparent medium. As for the $[DCA]^-$ ILs, the main feature in the FTIR spectrum was the strong characteristic absorptions of the –CN group in the $[DCA]^-$ ion ranging from 2134–2236 cm^{-1}. The spectrum of [S4]DCA shows (Figure 3a) three strong absorptions of the $[DCA]^-$ ion at 2135, 2195, and 2235 cm^{-1}. Moreover, the absorptions in the fingerprint region (523 and 663 cm^{-1} in Figure 3a) were assigned to the bending vibration resulting from the $[DCA]^-$ ion.

ESI-MS: Although ILs are always denoted as liquid salts composed entirely of ions, there is clear experimental evidence showing that a lot of cation–anion pairs and larger charged and neutral ion clusters exist in most ILs.[28,36] Undoubtedly, knowledge of the electrostatic interactions and supramolecular assembly behavior of ILs by atmospheric-pressure chemical ionization mass spectrometry (APCI-MS)[37] atmospheric-pressure thermal desorption ion mass spectrometry (APTDI-MS),[38] and electrospray ionization mass spectrometry (ESI-MS),[39] will be of great value for understanding intrinsically the ionic nature of ILs, and is therefore fundamental to understanding their unique properties. Herein, experimental evidence resulting from ESI-MS studies is provided, giving important information about the structural organization of these cyclic sulfonium salts. Dilute methanol solutions of the ILs were used for ESI-MS and two representative positive-ion spectra are provided in Figure 4. For [S1]DCA, in addition to the observation of the parent cation $[S1]^+$ (*m/z* 103.0579), positively charged ion clusters (*m/z* 272.1158 for $[(S1)_2DCA]^+$, *m/z* 441.1627 for $[(S1)_3(DCA)_2]^+$, and *m/z* 610.1998 for $[(S1)_4(DCA)_3]^+$) and their isotope patterns can also be detected. These peaks, corresponding to the aggregates of cations and anions, are very consistent with the theoretical values, thus confirming their identities. The relative abundances of positively charged ion clusters in the ESI-MS spectrum for [S1]DCA (Figure 3a) indicated that the positively charged dimer cluster (*m/z* 272.1158) is more easily formed than the trimer cluster (*m/z* 441.1627) and the tetramer cluster (m/z = 610.1998), and is even more abundant than the dissociated cation $[S1]^+$ in [S1]DCA.

The ion cluster behavior of [S4]NTf_2 was also studied, and its ESIMS spectrum is shown in Figure 4b. Apart from the detection of charged $[S4]^+$ (*m/z* 145.1047), the charged ion clusters (*m/z* 570.0869, 995.0367, 1419.9098, etc.) were also observed, and the peak values are very consistent with the theoretical values. As for the relative abundances of different ions and clusters in [S4]NTf_2, although a distribution trend similar to [S1]DCA was obtained, the charged dimer cluster $[(S4)_2NTf_2]^+$ obviously dominates the spectrum (Figure 4b). In addition, the larger cluster $[(S4)_5(NTf_2)_4]^+$ (*m/z* 1844.7584) was also detected, although its signal was very weak in comparison with those of other smaller ion clusters. Combining the ESI-MS results with the fact that these cyclic sulfonium $[DCA]^-$ and $[NTf_2]^-$ salts have lower viscosities and high conductivities (detailed discussions will be provided in the following sections), we think that they may be forming supramolecular clusters of lower nuclearity (in both positive and negative modes), as observed for the imidazolium salts in solution[39] or even in the gas phase.[37a,38]

UV/Vis absorptions and fluorescence behavior: The UV/Vis absorptions of the new ILs were also studied, and representative spectra of four ILs (0.1 wt% IL in ethanol solution) were selected for comparison. Although it is not shown in Figure 5, for a given anion the ILs exhibited similar absorption characteristics, a feature attributed to the fact that the sulfonium cations contributed only extremely weak absorptions in the UV regions due to their lack of chromophore. The UV/Vis absorptions of the precursors [S1]I, [S2]I, and [S4]I also proved this point.

Moreover, according to the absorbance spectra, the absorption intensity decreased in the anionic order: $[Sac]^- > [NO_3]^- > [DCA]^- > [NTf_2]^-$. Since the absorption in the UV region is related to the excitation of π electrons, this means that the $[Sac]^-$ ion should be more easily excited than other anions under the same conditions. In Figure 5, although only 0.1 wt% [S2]Sac was dissolved in ethanol, the strong absorption of the solution can be observed below 300 nm, and the absorption tail extends beyond

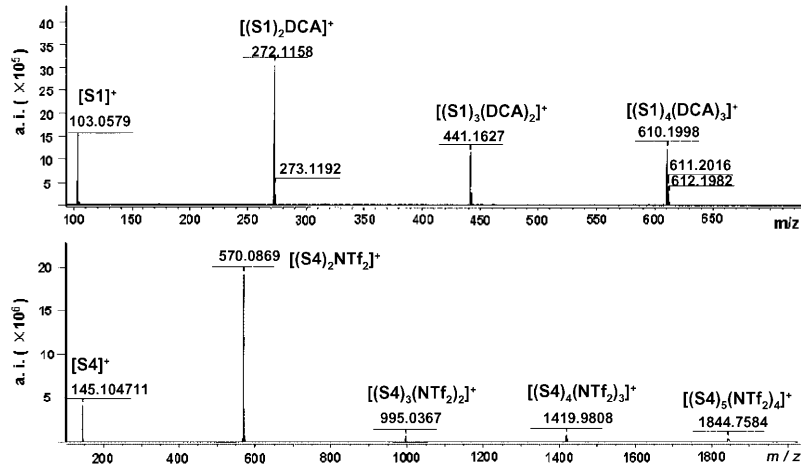

Figure 4. The positive-ion ESI mass spectra of [S1]DCA and [S4]NTf_2.

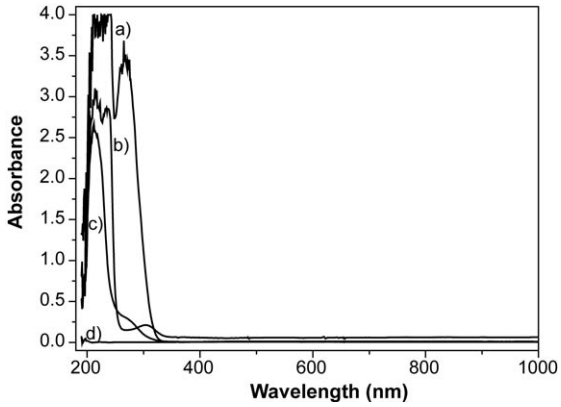

Figure 5. UV/Vis spectra of the ethanol solutions containing 0.1 wt % ILs. a)[S2]Sac, b) [S4]NO_3, c) [S2]DCA, d) [S4]NTf_2.

330 nm. However, almost no absorptions in UV/Vis regions occurred for the ethanol solution containing 0.1 wt % [S4]NTf_2, and the corresponding absorbance was less than 4.0 even when neat [S4]NTf_2 was employed, indicating that the absorption of this IL was comparatively weak. In comparison with the absorptions of [S2]Sac and [S4]NTf_2, the absorption intensity of $[DCA]^-$-based ILs was moderate, that is, weaker than that of [S2]Sac and stronger than that of [S4]NTf_2.

Figure 6 gives the emission spectra of six selected ILs (neat) at their maximum excited wavelengths. The results show that the fluorescence behavior of these sulfonium-based ILs is strongly dependent on the anion and there is only a little change resulting from the increase in the alkyl chain length of the cations. For four ILs with the $[S4]^+$ ion, the fluorescence intensity decreased in the order [S4]Sac > [S4]NTf_2 > [S4]DCA, and the strongest fluorescence of [S4]Sac was observed at 426 nm when the excited wavelength was 350 nm. The maximum excitation of [S4]NTf_2 occurred at 279 nm, much lower than those of other studied ILs. As for the three ILs with the $[DCA]^-$ ion, relatively strong emissions could be observed with excitation band ranging from 370–385 nm, and the maximum excited wavelengths of [S1]DCA, [S2]DCA, and [S4]DCA were 384 nm, 371 nm, and 373 nm, respectively. In addition, the fluorescence intensities of ILs with the $[DCA]^-$ ion were weaker than those of ILs with the $[NTf_2]^-$ or $[Sac]^-$ ions, which could be caused by the stronger π-conjugated system of $[Sac]^-$ or $[NTf_2]^-$ than $[DCA]^-$.

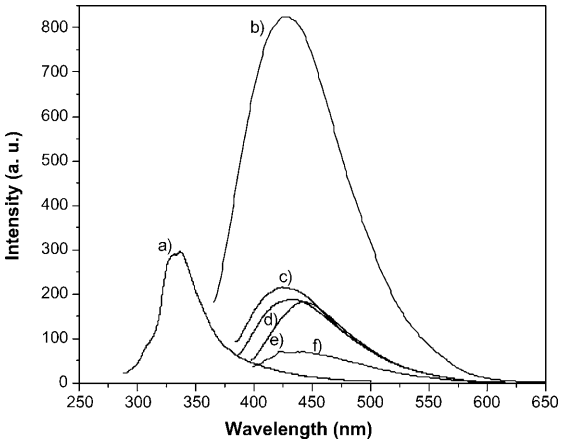

Figure 6. Emission behavior of six ILs at their maximum excited wavelengths, λ_{exc} (max, nm) = a) 279, [S4]NTf_2; b) 350, [S4]Sac; c) 373, [S4]DCA; d) 371, [S2]DCA; e) 384, [S1]DCA; f) 373, [S2]NO_3.

Moreover, the fluorescence behavior of pure ILs is strongly dependent on the excitation wavelength, as seen in Figure 7. For [S2]DCA, the fluorescence became very weak or could not be observed when the excited wavelengths were below 320 nm or over 480 nm. The fluorescence appeared at longer wavelength and became stronger in intensity with its emission band centered at 370 nm, and then the intensity decreased quickly with the maximum emission shifted to 491 nm from 406 nm as the excited wavelengths increased to 460 nm from 340 nm. Also, it is worth noting that no fluorescence was observed for any of the IL precursors (i.e., [S1]I, [S2]I, and [S4]I), whereas a strong intensity of > 6000 for NaSac, NaDCA, and $LiNTf_2$ was observed and only weak fluorescence was exhibited for $NaNO_3$. This indicates that the fluorescence behaviors of all sulfonium-based ILs are attributable mainly to the contribution of the anion and are independent of the sulfonium cations.

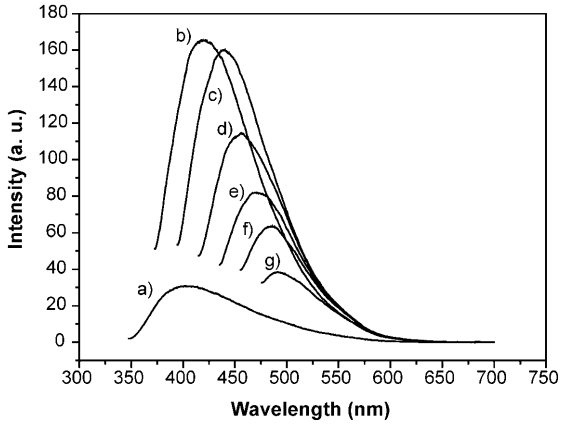

Figure 7. Excitation wavelength-dependent emission behavior of neat [S2]DCA. λ_{exc} (nm) = 340 (a), 360 (b), 380 (c), 400 (d), 420 (e), 440 (f), 460 (g).

Surface property: Surface property studies of ILs are particularly important for understanding many mechanisms involving interfacial chemistry of ILs, for example, biphasic homogeneous catalysis or supported IL phase catalysis. In comparison with the physicochemical "bulk" properties of ILs, XPS studies on ILs are relatively limited, but it has been proven that this technique is a powerful tool in the surface science of ILs.[40–42] Therefore, surface studies of these cyclic sulfonium-based ILs utilizing XPS were also per-

formed, and representative spectral information from two ILs ([S4]NTf_2 and [S2]DCA) is presented. Under our analysis conditions, both sulfonium-based ILs showed well-defined characteristic emissions, and no obvious degradation of the ILs was observed during or after measuring, which indicated that these sulfonium-based ILs are very stable during exposure to an X-ray source and ultra-high vacuum conditions.

Figure 8 shows the overview scan of a [S4]NTf_2 film and the high-resolution spectra for S 2p and C 1s. From the survey spectrum in Figure 8a, the expected elements F, N,

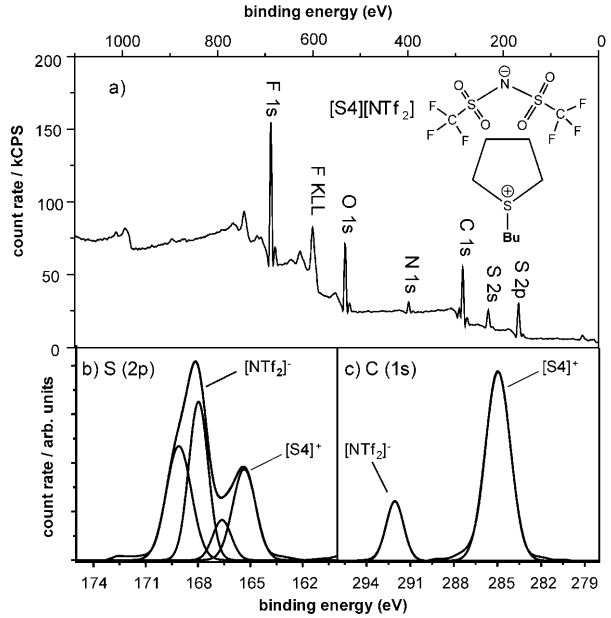

Figure 8. XPS spectra of [S4]NTf_2: survey spectrum (a) and high-resolution spectra (b, c) dealing with the S 2p, O 1s, and C 1s photoemission.

O, S, and C were all detected, and no evidence of impurities of other elements was found, indicating that the surface concentration of other impurities was below the detectable level for XPS. The electron emissions from N 1s, O 1s, F 1s, S 2p, and C 1s emissions all displayed well-resolved and narrow spectral features. For F 1s, N 1s, and O 1s, their 1s core level spectra were fitted with only one peak at the binding energies (B.E.) of 688.0 (F), 398.58 (N), and 531.8 eV (O), respectively. For sulfur, the S 2p signals originate from the two chemically different types of sulfur atoms in [S4]NTf_2, one from the cation and another from the anion. This is clearly reflected in the S 2p spectrum (Figure 8b). Furthermore, each S 2p signal can be fitted with two components due to the contribution of $2p_{1/2}$ and $2p_{3/2}$, respectively. The B.E. for the two types of S 2p peaks are 165.40 eV for S 2p in the $[S4]^+$ ion and 168.14 eV for S 2p in the $[NTf_2]^-$ ion. The atomic ratio of S and N is 3.1:1 (the theoretical ratio is 3:1), suggesting that the actual distribution of the $[S4]^+$ ion and the $[NTf_2]^-$ ion at the IL surface is close to 1:1. As shown in the C 1s spectrum (Figure 8c), at least two peaks are clearly distinguishable by their binding energies: one peak at 292.02 eV originating from CF_3 in the $[NTf_2]^-$ ion, and another peak at 285.00 eV, which can be assigned to eight carbon atoms in the $[S4]^+$ ion. Although there are at least three different chemical shifts for the eight carbon atoms in the cation, considering their similar binding energies, we are reluctant to make any further interpretation of the C 1s signal at 285.00 eV. According to the XPS intensities of various elements, we deduced the atomic ratio of five elements as follows: N:S:O:F:C = 1:3.1:4.7:6.4:11.3 (the theoretical ratio is 1:3:4:6:10). Clearly, the intensities of C and O are higher than the theoretical values, which may be caused by trace organic contaminations introduced during synthesis. In addition, the presence of Si-containing surface contaminants might also contribute to the excessive oxygen concentration,[43] although no Si signal was detected (possibly <0.3 wt%). The enrichment of F in the IL surface can be explained by the facts that fluorine has a high relative sensitivity factor (RSF = 1), and that the atoms of fluorine-containing anions involved in emissive processes are not affected by shake-up/off events.[44]

Figure 9a gives the XPS spectra of [S2]DCA, which are free from O and F. Besides the IL-related signals (C, S, and N), we observed trace Si-containing contaminants, which

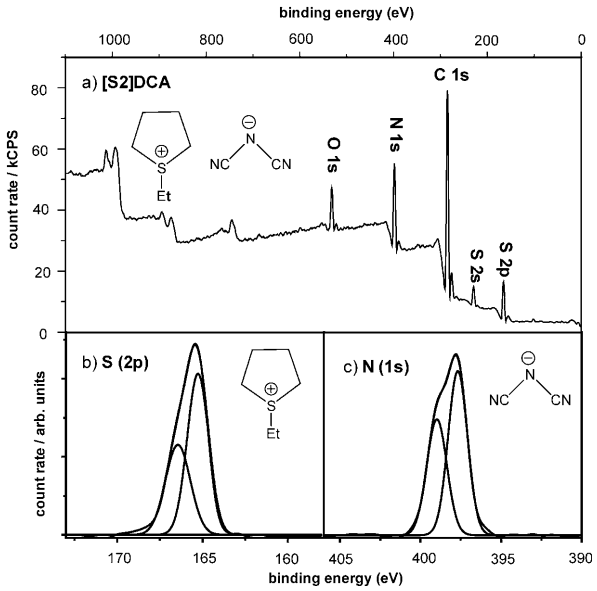

Figure 9. XPS spectra of [S2]DCA: survey spectrum (a) and high-resolution spectra (b, c) dealing with the S 2p and N 1s photoemission.

might originate from the sealing of the storage container or the silicone grease introduced during synthesis.[43,44] The S 2p spectrum of [S2]DCA is shown in Figure 9b. The B.E. of S $2p_{3/2}$ is 165.38 eV, which is assigned to the sulfur atom in the $[S2]^+$ ion. The high-resolution profile of the N 1s peak is shown in Figure 9c. It is clear that this photoemission consists of two resolved peaks, one peak at 398.97 eV for the nitrogen atom with the negative charge, and one peak at 397.69 eV for the nitrogen atom of the −CN group in $[DCA]^-$. In addition, the B.E. of O 1s in [S2]DCA is

531.68 eV, suggesting that it is very close to the chemical state of the O species in [S4]NTf_2 (B.E. is 531.8 eV). Although the nature of the impurities is not clear yet, it is likely that the excessive O and C signals in the XPS of [S2]DCA also originate in part from organic contamination introduced during synthesis. Similarly, the XPS spectra for other cyclic sulfonium-based ILs give well-defined characteristic photoemissions, indicating that XPS can indeed give large amounts of surface information for these novel liquids.

Phase behavior, melting point, and glass transition temperature: The solid–solid or solid–liquid phase transitions for these sulfonium salts were investigated by differential scanning calorimetry (DSC), and the data for melting points (T_m), freezing points (T_f), glass phase transition (T_g), solid–solid transition (T_{s-s}), and entropy change (ΔS_m), if appropriate, are collected in Table 1. In general, four types of phase transition behavior were observed for these cyclic sulfonium-based salts. Typical DSC traces for these four types of behavior are shown in Figure 10.

Table 1. Physical and thermal properties of cyclic sulfonium-based ILs.

Entry	Salts	T_g[a] [°C]	T_f[b] [°C]	T_{s-s}[c] [°C]	T_m[d] [°C]	C_p[e] [J g^{-1} K^{-1}]	T_d[f] [°C]
1	[S1]DCA		−19		13	2.00	179
2	[S2]DCA	−88				1.83	189
3	[S4]DCA	−80				1.87	187
4	[S1]NTf_2		85	−14, 16	98	2.08[h]	308
5	[S2]NTf_2		51	−19	69	1.73	298
6	[S4]NTf_2	−82				1.60	283
7	[S1]Sac	−43				2.01	161
8	[S2]Sac	−53				1.89	159
9	[S4]Sac	−33				1.86	168
10	[S1]NO_3		108	−29, −6	116	2.01	179
11	[S2]NO_3	−80	−15[g]		18	1.59	172
12	[S4]NO_3		23	−35, 20	54	1.83[h]	171

[a] Glass-transition temperature. [b] Freezing point. [c] Solid–solid transition. [d] Melting point. [e] Heat capacity at 25 °C. [f] Thermal decomposition temperature. [g] Cold-crystal temperature. [h] The sample was measured at 30 °C.

The first type of behavior is characterized by [S1]DCA, which has a single melting transition (Figure 10a, entry 1 in Table 1). The second type of behavior is represented by four salts that exhibited one or two solid–solid transitions (T_{s-s}) before melting (Figure 10b and c, entries 4, 5, 10, and 12 in Table 1). For example, two solid–solid transitions were observed for [S1]NTf_2 at −14 °C and 16 °C, respectively, before final melting at 98 °C, indicating a progressive transformation from a fully ordered state through a series of increasingly disordered phases. These solid–solid transitions, which are characteristic of plastic crystal, result from dynamically disordered orientations of IL constituents about the molecular axis.[8,45] Similarly, the salt [S2]NTf_2 also displayed the solid–solid transition, but only a single solid–solid transition could be observed before melting. The third type of behavior is represented by the salts that exhibited only a glass transition in a heating and cooling cycle without melting (entries 2, 3, and 6–9 in Table 1). From the DSC traces of this type, an obvious enthalpy relaxation during the glass transition could usually be observed (Figure 10d), indicating that these salts were not under thermodynamic equilibrium below T_g and therefore showed an endothermal phenomenon during glass transition to relax to equilibrium. The fourth type of behavior was observed only in [S2]NO_3 (Figure 10e). Here, only a glass transition occurred at −80 °C during cooling from 100 °C to −100 °C. However, upon heating, the salt first passed from the glass state to a subcooled phase at T_g, and then a cold crystallization occurred at −35 °C, followed by a preliminary melting at −5 °C and finally a full melting transition at 20 °C. In general, this phase behavior is dependent upon many factors and therefore is less predictable.

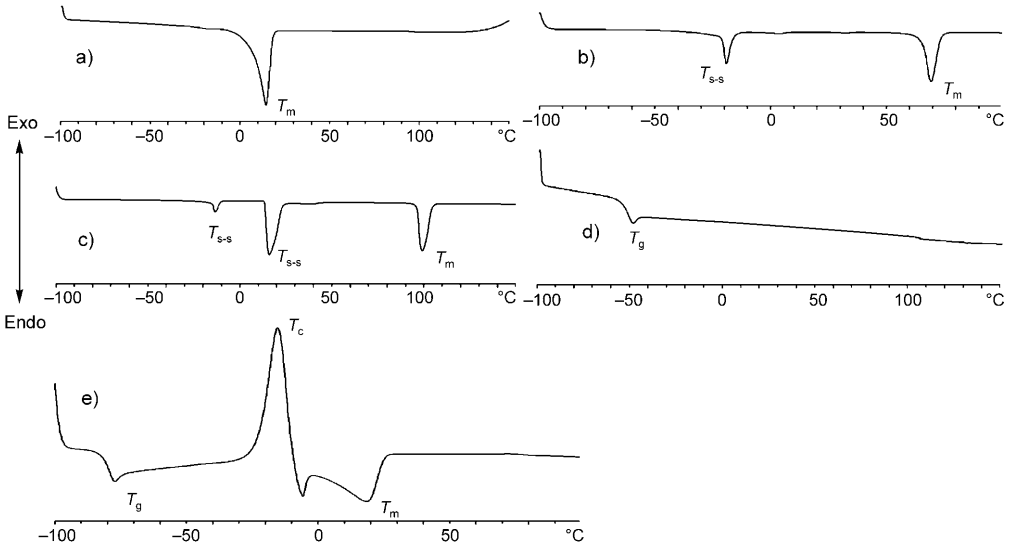

Figure 10. Representative DSC traces recorded at a rate of 10 °C min^{-1} in the heating process. a) [S1]DCA: single melting point (T_m); b) [S2]NTf_2: single solid-solid transition (T_{s-s}) before melting (T_m); c) [S1]NTf_2: two solid-solid transition (T_{s-s}) before melting (T_m); d) [S2]Sac: only glass transition (T_g); e) [S2]NO_2: glass transition (T_g) followed by crystallization (T_c), and melting (T_m).

Generally, the melting point (T_m) of an IL is determined mainly by the following three factors: molecular symmetry, intermolecular forces, and conformational degrees of freedom of the molecule.[46] For the twelve salts presented in this paper, except for [S1]NO_3 ($T_m = 116\,°C$) all the salts have a melting point of $< 100\,°C$ (some salts only displayed a glass transition and had no melting point). Obviously, the structure variation in the cation and anion has some impact on the melting point of these sulfonium salts. For a given anion, the T_m values generally increase in the order [S2] < [S4] < [S1], indicating that a medium cationic size might be beneficial to reducing ion symmetry and increase the ion's conformational degrees of freedom. In the family of salts containing the same cation, the T_m values are in the following anion order: $[DCA]^-$ < $[NTf_2]^-$ < $[NO_3]^-$. Since all three salts with the $[Sac]^-$ ion had no melting point during the temperature increase, the effect of the $[Sac]^-$ ion on T_m could not be compared with the salts based on other anions. From the above discussions, it can also be concluded that a medium cationic size combined with low symmetry and effective charge distribution in the anion favor destabilization of the packing efficiency in the crystal lattice of the ILs, thus decreasing their T_m values. However, no clear correlations are observed between the structures of these salts and their melting points.

The glass transitions of the new sulfonium-based ILs were also investigated. As seen in Table 1, seven sulfonium salts exhibited a glass transition, and the T_g values ranged from −88 to −33 °C. The structure of the anion clearly affected the T_g values of ILs. Among the developed ILs, the T_g values of the salts with the $[DCA]^-$ or $[NTf_2]^-$ ion are all ≤ −80 °C, much lower than for those with the large $[Sac]^-$ ion ($T_g = -53$ to 33 °C). This can be explained by the results derived from the bulky, non-fluorinated, rigid, and polarizable $[Sac]^-$ ion, that is, the relatively large size, high polarizability, and rigid structure as well as the non-fluorinated nature of $[Sac]^-$ ion enhances possible hydrogen bonding interactions between cation and anion, which in turn increases the T_g of the ILs. On the other hand, for ILs with a $[Sac]^-$ ion, the T_g values generally increase in the cationic order [S2] < [S1] < [S4], which is different from the trend observed for the effect of cationic structure on T_m. This also indicates that the influence of cationic structure on T_m comes from many factors, such as the strength of ion interactions, the ion size, as well as the flexibility and polarizability of the anion, and a medium cationic size might be helpful to decrease the T_g of ILs by means of weakening electrostatic interactions between cation and anion. For a given anion, no clear correlations are observed between the structure of the cation and the glass transition temperature.

Heat capacity and thermal stability: The heat capacities (C_p) of ten ILs at 25 °C were measured (Table 1), and the values range from 1.59–2.08 $J\,g^{-1}\,K^{-1}$. Since a solid–solid transition at about 25 °C occurred for [S1]NTf_2 and [S4]NO_3, their heat capacities were not measured. The data in Table 1 indicate that the ILs based on the [S1] cation have higher heat capacities ($\geqq 2.0\,J\,g^{-1}\,K^{-1}$) than those with other anions. For example, the heat capacities of [S1]Sac and [S1]NO_3 are both 2.01 $J\,g^{-1}\,K^{-1}$, which is even higher than thermal oil (1.907 $J\,g^{-1}\,K^{-1}$).

Moreover, the thermal stability of the salts was investigated by thermogravimetric analysis (TGA). As shown in Table 1, the temperatures of thermal decomposition (T_d, i.e., the temperatures at which the weight loss of a compound in an aluminum pan under an N_2 atmosphere reached 5 wt%) of the twelve salts employed in this work are in the range of 159–308 °C, which are lower than for 1,3-dialkylimidazolium-based ILs (in general, $T_d > 300\,°C$), and even lower than for the structurally related pyrrolidinium salts such as [$P_{1,2}$]DCA ($T_d = 250\,°C$).[47] As shown in Figure 11, the salts

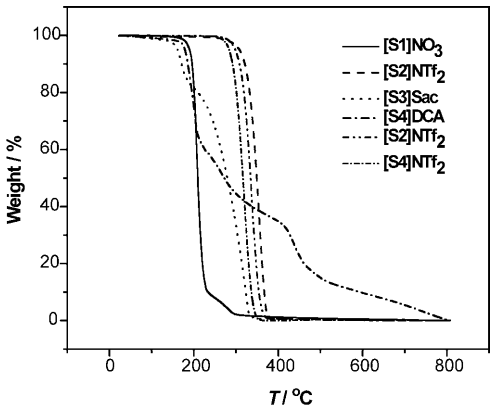

Figure 11. TGA traces of six cyclic sulfonium-based salts.

containing $[NTf_2]^-$ exhibited much higher thermal stability than those with the other three anions (i.e., $[DCA]^-$, $[Sac]^-$, and $[NO_3]^-$). Irrespective of the cations, the thermal stabilities of these salts generally increase in the order $[Sac]^-$ < $[NO_3]^-$ < $[DCA]^-$ < $[NTf_2]^-$. This trend indicates that the anion has a significant impact on the thermal stability of the sulfonium salts.

Density, viscosity, and refractive index: For the salts that are liquids at 25 °C, the fundamental properties including densities (ρ), viscosities (η), and refractive indices (n) were also measured, and the corresponding characterization data are presented in Table 2. The ρ values of eight RTILs lie in range of 1.098–1.472 $g\,cm^{-3}$. For a given anion, the densities of these cyclic sulfonium-based ILs decreased gradually with increasing formula weight (M_w) of the cation, which is attributed to the relatively smaller van der Waals volume of the cation along with the increase of the alkyl chain length. For the salts with the same cation, the ρ values decrease in the following anion order: $[DCA]^-$ < $[Sac]^-$ < $[NO_3]^-$. The ILs based on $[DCA]^-$ displayed relatively lower densities than ILs with other anions, and [S4]DCA gave the smallest ρ value (1.098 $g\,cm^{-3}$ at 25 °C), which is still slightly higher than the structurally related pyrrolidinium salts (e.g., $\rho = 0.92$, 0.95, and 0.92 $g\,cm^{-3}$ for [P_{13}]DCA, [P_{14}]DCA, and

Table 2. Density (ρ), viscosity (η), and refractive index (n) of eight sulfonium-based ILs.

ILs	Water content [ppm]	ρ[a] [g cm^{-3}]	Viscosity (η): ln η = ln A + E_η/RT (T in K)				n[c]
			H[b] [mPa s]	E_η [kJ mol^{-1}]	$10^4 A$ [mPa s]	R^2	
[S1]DCA	248.1	1.169	49.8	25.20	16.3	0.995	1.5502
[S2]DCA	297.2	1.135	34.2	25.23	14.5	0.991	1.5426
[S4]DCA	292.2	1.098	62.6	31.66	1.68	0.988	1.5315
[S4]NTf_2	50.3	1.456	104.8	36.44	0.39	0.991	1.4420
[S1]Sac	317.2	1.423	> 2000	–	–	–	1.5940
[S2]Sac	259.4	1.350	> 2000	–	–	–	1.5795
[S4]Sac	287.3	1.265	> 2000	–	–	–	1.5785
[S2]NO_3	384.7	1.472	156.8[d]	31.27	6.12	0.997	1.5401

[a] Density at 25 °C. [b] Viscosity at 20 °C. [c] Refractive index at 25 °C. [d] The sample was measured at 30 °C.

[P_{16}]DCA at 25 °C, respectively).[47] Because the effect of temperature on the IL's density is not as obvious as for the viscosity and conductivity, the temperature dependence of density was not investigated in this work.

The viscosities of the eight RTILs were measured. Except for the ILs with a $[Sac]^-$ ion, most cyclic sulfonium-based ILs showed relatively low viscosities (34.2–104.8 mPa s at 20 °C, Table 2), much lower than those of traditional 1,3-dialkylimidazolium $[BF_4]^-$ and $[PF_6]^-$ salts (e.g. $\eta = 112$ mPa s for [BMIm]BF_4 and $\eta = 201$ mPa s for [BMIm]PF_6 at 20 °C).[48] [S2]DCA had the lowest viscosity of all salts under investigation ($\eta = 34.2$ mPa s at 20 °C), even lower than for the pyrrolidinium $[DCA]^-$ salts ($\eta = 45$, 50, and 45 mPa s for [P_{13}]DCA, [P_{14}]DCA, and [P_{16}]DCA at 20 °C, respectively),[47] whereas the ILs based on the $[Sac]^-$ ion displayed high viscosities of >2000 mPa s at the same temperature. Moreover, the relationships between ion structure and viscosity were also noticeable. For a given anion, the viscosity decreases in the order $[S4]^+ > [S1]^+ > [S2]^+$, for example, the viscosities of [S4]DCA, [S1]DCA, and [S2]DCA are 62.6, 49.8, and 34.2 mPa s, respectively. In comparison with the inconspicuous impact induced by cationic variation, the effect of the anion on the viscosity is remarkable. Obviously, the $[DCA]^-$ ILs had much lower viscosities than the ILs with other anions. For example, the η value of [S4]DCA is only 62.6 mPa s at 20 °C, but the η value of [S4]NTf_2 reaches 104.8 mPa s at the same temperature. The low viscosities of the $[DCA]^-$ ILs may be explained by the increased ion mobility owing to smaller anion size and better charge delocalization in $[DCA]^-$ than other anions. Although the $[Sac]^-$ ion also possesses good charge distribution, extremely high viscosities (>2000 mPa s at 20 °C) were observed for all $[Sac]^-$ salts, which could be attributed to high rigidity (comprising two conjugated rings) and strong ion interactions (mainly van der Waals interactions induced by the C=O group and two S=O groups), and the larger size of the $[Sac]^-$ ion.

The temperature dependence of viscosity was investigated for five ILs over the temperature range −20 to 80 °C, and the Arrhenius plots of viscosity according to Equation (1) are shown in Figure 12.

$$\ln\eta = \ln A + E_\eta/RT \quad (1)$$

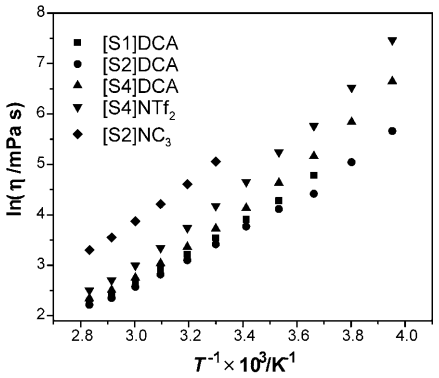

Figure 12. Arrhenius plot of viscosity for five sulfonium salts.

E_η is the activation energy for viscous flow, which is always regarded as the energy barrier to be overcome by ions to move past each other, and thus its value is correlated with the structure of both cation and anion. The values of E_η, A, and the linear fitting parameter (R^2) for all the ILs are calculated and listed in Table 2. According to the values of R^2 in Table 2, the five salts were approximately fit by the Arrhenius model over the temperature range −20 to 80 °C. In comparison with the $[S4]^+$ salts, [S1]DCA, and [S2]DCA gave relatively smaller E_η values (25.20 and 25.23 kJ mol^{-1}, respectively), indicating that both ILs have a lower energy barrier and thus exhibit lower viscosity.

The refractive indices (n) of eight sulfonium-based salts at 25 °C ranged from 1.4420–1.5940 (Table 2), higher than those of the traditional dialkylimidazolium $[BF_4]$ and $[PF_6]$ salts (e.g., $n = 1.4188$ for [BMIm]BF_4 and $n = 1.4083$ for [BMIm]PF_6 at 25 °C).[49] Similarly to the viscosity, the structure variation in the cation and anion has some impact on the refractive indices of ILs. In general, for the same cation, the high refractive indices of the ILs reflect particularly high electron mobility in the anion. Among the studied ILs, the refractive indices decreased in the order $[Sac]^- > [DCA]^- > [NO_3]^- > [NTf_2]^-$, and [S1]Sac gave the highest refractive index (1.5940). The cationic structure also influences the refractive indices of the salts. For the same anion, the refractive indices increase with increasing chain length of the cations. The effect of temperature on the refractive index was also studied (Figure 13), and the n values decreased linearly with increasing temperature. As the curve shows, the attenuation slope of the eight lines is approximate. This means that although the cationic or anionic structures of the eight salts were different, the effect of the temperature on the refractive index was almost the same.

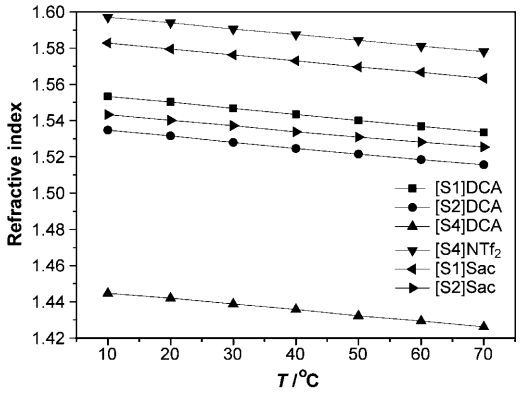

Figure 13. Refractive indices of eight ILs as a function of temperature.

Tribological properties: The ILs were found to possess excellent tribological properties, and thus could be used as valuable lubricants. However, very few studies on the tribological performance of sulfonium-based ILs have been reported so far. Many S-containing compounds, such as MoS_2, have been proven to be good solid lubricants. Therefore, the tribological performance of novel cyclic sulfonium-based ILs as lubricants for various sliding contacts was also evaluated in this work.

For the purpose of comparison, a typical IL [BMIm]NTf_2 was also employed. From the test results of friction and wear of various ball-on-disc systems lubricated with four studied ILs as lubricants (Table 3), it is found that the structure of the IL has some impact on its tribological performance. In comparison with [BMIm]NTf_2, [S4]NTf_2 showed much lower friction coefficients; that is, [S4]NTf_2 has better tribological properties than [BMIm]NTf_2. For [S4]DCA, much lower friction coefficients than [BMIm]NTf_2 were obtained in steel/Cu and Si_3N_4/Cu tests, but only similar tribological performance to [BMIm]NTf_2 was observed in steel/steel and steel/Al tests. As for [S2]Sac, poor wearing performance was observed in steel/steel, steel/Al, and Si_3N_4/Cu tests. However, the friction coefficient of [S2]Sac in the steel/Cu test was 0.13, much lower than the 0.22 for [BMIm]NTf_2, that is, [S2]Sac showed better tribological properties than [BMIm]NTf_2 when tested for the steel/Cu system, although the detailed mechanism is still not clear at this stage.

Table 3. Friction coefficients for different frictional pairs lubricated with four ILs.[a]

Frictional pair (ball/disk)	Friction coefficient			
	[S2]Sac	[S4]NTf_2	[BMIm]NTf_2	[S4]DCA
steel/steel	0.15	0.13	0.15	0.15
steel/Al	0.16	0.14	0.13	0.13
steel/Cu	0.13	0.15	0.22	0.12
Si_3N_4/Cu	0.20	0.13	0.15	0.11

[a] SRV tester, load 200 N, frequency 25 Hz, amplitude 1 mm.

Conductivity and electrochemical stability: The conductivity of an IL is of vital importance if it is to be considered as a supporting electrolyte in electrochemical devices. According to the conclusions drawn by Grätzel et al.,[6] the ionic conductivity (κ) of an IL should be related to its viscosity (η), formula weight (FM), and density (ρ), and the radii of its cation and anion (r_c and r_a), as described by Equation (2), in which $0<y<1$ is the degree of dissociation, F is the Faraday constant, ζ_a and ζ_c are the anion and cation microviscosity factors, respectively.

$$\kappa = yF^2\rho/(6\pi N_A FW\eta)[(\zeta_a r_a)^{-1} + (\zeta_c r_c)^{-1})] \quad (2)$$

Therefore, besides the obvious influence of the viscosity, the effect of ion size and weight must be stressed. In the search for highly conductive ILs, one must not focus on viscosity only, but keep in mind the importance of ion size. Figure 14 shows the temperature dependence of the specific conductivities (κ) for four representative ILs based on $[DCA]^-$ and $[NTf_2]^-$ in the temperature range from −30 to 80 °C. At 20 °C, the ionic conductivities of four examined ILs range from 3.2 to 17.6 mS cm^{-1} (Table 4). [S2]DCA displayed the highest conductivity (17.6 mS cm^{-1} at 20 °C), even higher than that of [EMIm]BF_4 (14 mS cm^{-1} at 20 °C).[49] From Figure 14, it is clear that the conductivities were more

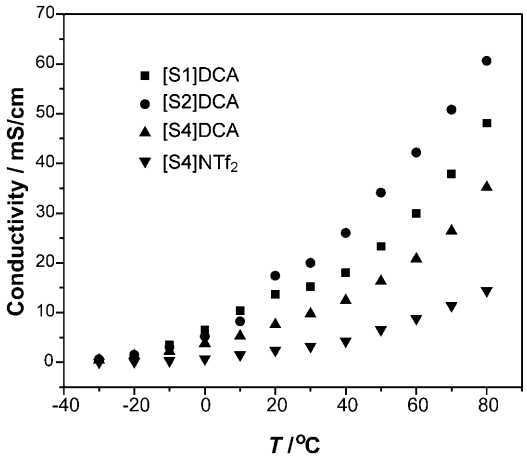

Figure 14. Change of ion conductivity with increasing temperature for new ILs.

Table 4. Electrochemical properties of four selected ILs with low viscosities

ILs	Reductive voltage [V]	Oxidative voltage [V]	Electrochemical window [V]	Conductivity[a] [mS cm^{-1}]
[S1]DCA	−1.8	1.4	3.2	13.6
[S2]DCA	−1.8	1.4	3.2	17.6
[S4]DCA	−1.8	1.4	3.2	7.6
[S4]NTf_2	−1.8	2.0	3.8	3.2

[a] Conductivities were measured at 20 °C.

affected at high temperature. The reason might be that at low temperatures the κ value is strongly affected by viscosity, and at high temperature the intrinsic structure and characteristics of the ILs may determine the κ value. Similarly to the viscosity, the structure of cation and anion has some effect on the conductivities. For the same anion, the conductivity values of anions are in the following order: $[S4]^+ < [S1]^+ < [S2]^+$. This is contrary to the viscosity order of cations; for a given cation, the $[DCA]^-$ ILs have much higher conductivities than the ILs with other anions, for example, at 20 °C [S4]DCA exhibits a conductivity of 7.6 mS cm^{-1}, but the κ value of $[S4]NTf_2$ is only 3.2 mS cm^{-1}. This can be explained by the lower viscosity and smaller anion size of the former, which can improve the rate of ion mobility.

The electrochemical stability of most of the ILs was evaluated by cyclic voltammetry. Figure 15 shows a typical cyclic voltammetry curve for $[S4]NTf_2$. Compared to the conventional 1,3-dialkylimidazolium-based ILs (e.g., EW = 3.5 V for [EMIm]DCA and 4.1 V for $[EMIm]NTf_2$),[10b,27a] these cyclic sulfonium-based salts exhibited lower electrochemical stabilities, and their electrochemical windows (EWs) ranged only from 3.2–3.8 V (Table 4). For [S1]DCA, [S2]DCA, and [S4]DCA, an approximate reductive potential was observed at −1.8 V, which meant that the electrochemical stabilities of the cations were influenced very little by the alkyl substitution pattern in the IL's cation. Moreover, by comparing the oxidative potentials of $[S4]NTf_2$ and [S4]DCA, it was found that the oxidative voltage of 2.0 V for $[NTf_2]^-$ was obviously higher than 1.4 V for $[DCA]^-$, indicating that the $[DCA]^-$ ion was more easily oxidized than the NTf_2^- ion. Moreover, one remarkable characteristic for $[S4]NTf_2$ is that no obvious oxidation peak appeared at 2.0 V (i.e. the oxidative potential of the anion, Figure 15), which can be explained by the passivation of the anodic electrode induced by the trace S-containing contaminations during cyclic voltammetry. Similar phenomena could also be observed for the electrochemical behaviors of three $[DCA]^-$ ILs.

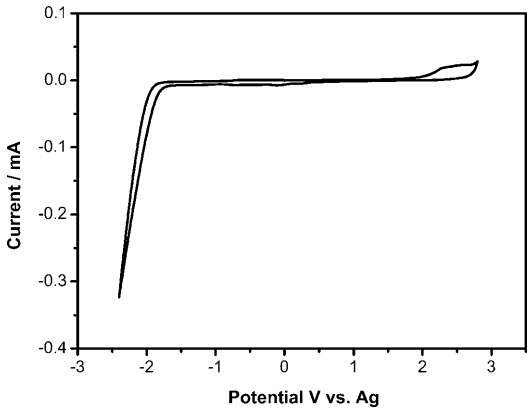

Figure 15. Cyclic voltammogram of $[S4]NTf_2$; GC working electrode.

Conclusion

A novel family of cyclic sulfonium-based ILs has been prepared and characterized. Their physicochemical properties, including molecular vibrations, UV/Vis absorptions, fluorescence behavior, ion aggregation behavior, surface properties, thermal properties, densities, viscosities, refractive index, tribological property, and electrochemical properties, have been studied in detail. Among twelve developed ILs, eight of them are liquids at room temperature. The $[DCA]^-$-based ILs exhibit much lower viscosities (34–62 mPa s at 20 °C) than most 1,3-dialkylimidazolium $[BF_4]^-$ and $[PF_6]^-$ salts (> 100 mPa s at 20 °C). Four of the ILs exhibit organic plastic crystal behavior, and to our knowledge, no example of IL materials based on sulfonium salts has been previously reported to possess this characteristic. $[S4]NTf_2$ has almost no absorptions in the 1352–2880 cm^{-1} IR region and only weak absorption in the whole UV region. ILs based on the $[Sac]^-$ ion display high refractive indices (1.5785–1.5940 at 20 °C) owing to the high electron mobility of $[Sac]^-$. In addition, some ILs with the $[NTf_2]^-$ and $[Sac]^-$ ion show better tribological performance than $[BMIm]NTf_2$ in the steel/Cu wearing test, and those $[DCA]^-$-based ILs show much higher conductivities (7.6–17.6 mS cm^{-1} at 20 °C) than most traditional 1,3-dialkylimidazolium salts. Hence, these new sulfonium salts could be promising electrolytes for electrochemical devices and good potential lubricants.

Experimental Section

General: Commercially available regents were purchased from Aldrich, Tianjin Chemical Reagent Corporation Ltd., or Alfa Aesar Inc., were of analytical grade and were used in this work as received.

NMR, FTIR, and ESI-MS: Before NMR, FTIR and ESI-MS analyses, each sample was obtained by filtration through a silica column, and dried at 90–100 °C and 10^{-2}–10^{-3} mbar for 4 h. ^{1}H NMR spectra were recorded on a Bruker AMX FT 400 MHz NMR spectrometer. Chemical shifts were reported downfield in parts per million (ppm, δ) from a tetramethylsilane reference. IR spectra were recorded on a Thermo Nicolet 5700 FTIR spectrophotometer. Electrospray ionization mass spectra were recorded on a Bruker Daltonics APEX II 47e FTMS. The samples were dissolved in methanol.

UV/Vis, fluorescence, and XPS: UV/Vis spectra were conducted on an Agilent 8453 UV/Vis spectrophotometer, and the fluorescence spectra were recorded at room temperature on a Hitachi model F-7000 FL spectrophotometer at a scan speed of 1200 nm min^{-1}. Before both UV/Vis and fluorescence analysis each sample was dried at 90–100 °C and 10^{-2}–10^{-3} mbar for 4 h. The sample were contained in 1 cm quartz cuvettes during measurements, and were measured in open ambient conditions within 1–3 min. X-Ray Photoelectron Spectroscopy (XPS) analyses were performed on a VG ESCALAB 210 instrument with $Mg_{K\alpha}$ source (1253.6 eV) and calibrated versus the C 1s peak at 285.0 eV. A thin layer of IL was deposited on a polycrystalline gold substrate, and was kept under moderate vacuum for at least 12 h before introduction into the analytical chamber of the XPS instrument. Spectrometer pass energies of 100 eV for the survey spectra and 30 eV for high resolution spectra were used for all elemental spectral regions. The pressure in the analyser chamber was 10^{-9} Torr.

Water content: The water content in ILs was detected by means of a coulometric Karl–Fischer titration using a Mitsubishi CA-06 Moisturemeter, and each test was conducted in an anhydrous sealed chamber and was

finished within 1 min. Duplicate measurements were performed on each sample with results agreeing to within 5%. Before the water content test, each sample were kept at 90°C and 10^{-2}–10^{-3} mbar for 4 h, except for the ILs based on the $[NTf_2]^-$ ion, which were dried at 100°C.

Phase transitions and thermal stability: Measurements of glass-transition temperatures, melting and freezing points, and heat capacities were carried out on a Mettler–Toledo differential scanning calorimeter (DSC), model DSC822^e, and the data were evaluated by using the Mettler–Toledo STARe software version 7.01. The instrument was calibrated for temperature and heat flow with zinc and indium reference samples provided by Mettler–Toledo. Samples were placed in a 40 μL hermetically sealed aluminum pan with a pinhole at the top of the pan. An empty aluminum pan was used as the reference. The samples inside the differential scanning calorimeter furnace were exposed to a flowing N_2 atmosphere. Before the DSC test, each sample was dried at 90–100°C and 10^{-2}–10^{-3} mbar for 4 h, and was further dried in situ on the differential scanning calorimeter by holding the sample at 120°C for 15 min. This is important because the presence of volatiles, especially water, can affect the glass-transition and melting temperatures. Melting, crystallization, and glass-transition temperatures were determined by cooling the samples from 150°C to −100°C, followed by heating from −100°C to 150°C, both at a rate of 10°C min^{-1}. The glass-transition temperature was determined as the midpoint of a heat capacity change, whereas the melting and crystallization temperatures were determined as the onset of the transition. The decomposition temperature (T_d) was recorded with 10% of mass loss by using a Pyris Diamond Perkin-Elmer TG/DTA with scan rate of 20°C min^{-1} under a N_2 atmosphere, and the samples for TG/DTA measurements were sealed tightly in Al_2O_3 pans. Each sample before the TGA test was also dried at 90–100°C and 10^{-2}–10^{-3} mbar for 4 h.

Measurement of the viscosity, density, and refractive index: The viscosity of each IL was measured on a Stabinger Viscosimeter SVM 3000/GR. The density was examined by the weight method at 25°C. Measurements of refractive indices were conducted with a WAY-2s Abbe refractometer (Shanghai Precision & Scientific Instrument Co.), calibrated by the refractive indices of deionized water. Each sample, before viscosity, density, and refractive index analyses, underwent removal of water as before the test of water content. For these three analyses, all the samples were measured in an open ambient atmosphere and each test at a specified temperature was conducted within 1–3 min.

Conductivity and electrochemical stability: The ion conductivity was measured by using a Mettler–Toledo Seven Muliti meter, and the sample underwent removal of water as before the test of water content. Similarly to the viscosity and refractive index, the IL conductivities were measured under open ambient conditions and each measurement at a specified temperature was completed within 1–3 min. Cyclic voltammetry was conducted by using a CHI 660A Electrochemical Work Station. The working electrode was a glassy carbon electrode (3 mm diameter) and the auxiliary electrode was a platinum wire. The reference electrode was Ag/AgCl, and porous glass frits were used to separate the internal solutions from the working solutions and 3 M KCl solution. Before testing, each sample was kept at 90°C and in a vacuum at <5 mm Hg for 1 h. Electrolysis was carried out in a conventional three-electrode electrochemical cell equipped with a sealed chamber with which temperatures could be monitored and adjusted from room temperature to about 90°C through a circular water bath system, and vacuum treating ($\approx$1 mm Hg) and N_2 filling could also be implemented so as to minimize the influence of O_2 and H_2O during experiments.

Tribological coefficient: Before the tribological test, each sample underwent removal of water as before the test of water content. The tribological coefficients of the selected ILs were evaluated by using an Optimol SRV (SRV is the abridged name for German Schwingung, Beibung, Verschleiss) oscillating friction and wear tester. The friction and wear tests were performed at room temperature in a ball-on-disc configuration, by oscillating an AISI52100 alloy steel ball (or Si_3N_4 ball) over a steel, Al, or Cu block at a frequency of 25 Hz, with a sliding amplitude of 1 mm. Prior to the friction and wear test, two drops of the lubricant were let into to the ball–disc contact area. The friction coefficient curve was recorded automatically with a chart attached to the SRV test rig.

General procedure for cyclic sulfonium iodides: The desired cyclic sulfonium iodide precursors were synthesized according to an approach similar to that reported previously.[32,33,35] A solution of tetrahydrothiophene (44.0 g, 0.50 mol) in dry acetone (200 mL) was prepared. A small excess of alkyl iodide (0.55 mol) was added slowly and the resulting mixture was stirred vigorously in darkness at room temperature for several days. The white precipitate produced was removed by filtration and the filter cake was washed with anhydrous diethyl ether. The resulting solid was dried in clean and dry reagent bottles under reduced pressure for 2 h. The purified product was wrapped in aluminum foil and stored in a desiccator under dry nitrogen.

[S1]I: White solid, yield: 91%; MW, 229.96. ^{1}H NMR (DMSO, 500 MHz): $\delta=3.44$ (m, 2H), 3.26 (m, 2H), 2.75 (s, 3H), 2.21 (m, 2H), 2.10 ppm (m, 2H); IR: $\tilde{\nu}=2984$, 2938, 2875, 1460, 1424, 1401 cm^{-1} (ν_{C-H} aliphatic); MS (ESI$^+$) calcd: m/z: 103.06 ($[C_5H_{11}S]^+$); found: m/z: 103.0579.

[S2]I: White crystal, yield: 85%; MW, 243.98. ^{1}H NMR (DMSO, 500 MHz): $\delta=3.45$ (m, 2H), 3.37 (m, 2H), 3.21 (m, 2H), 2.18 (m, 2H), 2.11 (m, 2H), 1.29 ppm (t, 3H); IR: $\tilde{\nu}=2948$, 2875, 1450, 1416, 1385 cm^{-1} (ν_{C-H} aliphatic); MS (ESI$^+$) calcd: m/z: 117.07 ($[C_6H_{13}S]^+$); found: m/z: 117.0734.

[S4]I: White crystal, yield: 64%; MW, 272.01. ^{1}H NMR (DMSO, 500 MHz): $\delta=3.47$ (m, 2H), 3.37 (m, 2H), 3.18 (m, 2H), 2.22 (m, 2H), 2.11 (m, 2H), 1.64 (m, 2H), 1.36 (m, 2H), 0.88 ppm (t, 3H); IR: $\tilde{\nu}=2954$, 2931, 2869, 1463, 1409 cm^{-1} (ν_{C-H} aliphatic); MS (ESI$^+$) calcd: m/z: 145.1 ($[C_8H_{17}S]^+$); found: m/z: 145.1047.

General procedure for cyclic sulfonium salts with $[NTf_2]^-$ ions: The produced cyclic sulfonium iodide precursors and lithium bis(trifluoromethylsulfonyl)imide ($LiNTf_2$, $\geq$99.95%, Aldrich), were dissolved in deionized water and mixed for 2 h at ambient temperature (a 1:1.1 molar ratio of iodide/$LiNTf_2$ was employed to ensure the metathesis reaction ran as completely as possible). The crude products (solid precipitates or liquid) were separated from water, followed by thorough washing with deionized water until no residual iodide anions in the deionized water were detected by use of $AgNO_3$. The final products were dried under high vacuum for more than 4 h at 100°C, and then were wrapped in aluminum foil and stored in a desiccator under dry nitrogen.

[S1]NTf$_2$: White crystal, yield: 94%; MW, 382.96. ^{1}H NMR (CD_3COCD_3, 500 MHz): $\delta=3.79$ (m, 2H), 3.61 (m, 2H), 3.05 (s, 3H), 2.51 (m, 2H), 2.42 ppm (m, 2H); IR: $\tilde{\nu}=3033$, 2964, 2892, 1432 (ν_{C-H} aliphatic), 1354, 1194, 1137, 1056, 794, 741 cm^{-1}; MS (ESI$^+$) calcd: m/z: 103.06 ($[C_5H_{11}S]^+$); found: m/z: 103.0579.

[S2]NTf$_2$: White solid, yield: 93%; MW, 396.98. ^{1}H NMR (CD_3COCD_3, 500 MHz): $\delta=3.78$ (m, 2H), 3.66 (m, 2H), 3.47 (m, 2H), 2.49 (m, 2H), 2.39 (m, 2H), 1.54 ppm (t, 3H); IR: $\tilde{\nu}=2985$, 2959, 2888, 1457 (ν_{C-H} aliphatic), 1352, 1194, 1140, 1059, 790, 740 cm^{-1}; MS (ESI$^+$) calcd: m/z: 117.07 ($[C_6H_{13}S]^+$); found: m/z: 117.0734.

[S4]NTf$_2$: Colorless liquid, yield: 89%; MW, 425.02. ^{1}H NMR (DMSO, 500 MHz): $\delta=3.79$ (m, 2H), 3.66 (m, 2H), 3.44 (t, 2H), 2.50 (m, 2H), 2.44 (m, 2H), 1.91 (m, 2H), 1.56 (m, 2H), 0.96 ppm (t, 3H); IR: $\tilde{\nu}=2967$, 2940, 2879, 1468 (ν_{C-H} aliphatic), 1352, 1194, 1140, 1059, 790, 740 cm^{-1}; MS (ESI$^+$) calcd: m/z: 145.1 ($[C_8H_{17}S]^+$); found: m/z: 145.1048.

General procedure for cyclic sulfonium salts with $[DCA]^-$, $[NO_3]^-$, and $[Sac]^-$ ions: An aqueous solution of the cyclic sulfonium iodides was added to aqueous slurry of the excess silver salts containing the target anion (1:1.1 molar ratio for AgDCA/iodide and AgSac/iodide, and 1:1 molar ratio for $AgNO_3$/iodide) and the solution was heated to 40°C with stirring for 4 h. Silver iodide was removed from the solutions by filtration. After complete removal of water, the resulting viscous liquids or solids were washed with diethyl ether under vigorous stirring three times and the volatile component removed. To ensure complete removal of silver salts from the product, the dried products were dissolved in dry dichloromethane or acetone and cooled in a freezer overnight before further filtration. The final products were dried under high vacuum for more than 4 h at 100°C, and then were wrapped in aluminum foil and stored in a desiccator under dry nitrogen.

[S1]DCA: Colorless liquid, yield: 93%; MW, 169.07. ^{1}H NMR (CD_3COCD_3, 500 MHz): δ=3.78 (m, 2H), 3.60 (m, 2H), 2.92 (m, 3H), 2.55 (m, 2H), 2.42 ppm (m, 2H); IR: $\tilde{\nu}$=2953, 2884 (ν_{C-H} aliphatic), 2236, 2196, 2135 cm^{-1} ($\nu_{C=N}$); MS (ESI$^+$) calcd: *m*/*z*: 103.06 ($[C_5H_{11}S]^+$); found: *m*/*z*: 103.0579.

[S2]DCA: Colorless liquid, yield: 92%; MW, 183.08. ^{1}H NMR (CD_3COCD_3, 500 MHz): δ=3.75 (m, 2H), 3.65 (m, 2H), 3.46 (m, 2H), 2.48 (m, 2H), 2.41 (m, 2H), 1.53 ppm (t, 3H); IR: $\tilde{\nu}$=2977, 2950, 2884 (ν_{C-H} aliphatic), 2234, 2195, 2134 cm^{-1} ($\nu_{C=N}$); MS (ESI$^+$) calcd: *m*/*z*: 117.07 ($[C_6H_{13}S]^+$); found: *m*/*z*: 117.0734.

[S4]DCA: Colorless liquid, yield: 90%; MW, 211.11. ^{1}H NMR (CD_3COCD_3, 500 MHz): δ=3.76 (m, 2H), 3.64 (m, 2H), 3.43 (t, 2H), 2.49 (m, 2H), 2.40 (m, 2H), 1.88 (m, 2H), 1.53 (m, 2H), 0.97 ppm (t, 3H); IR: $\tilde{\nu}$=2962, 2937, 2875 (ν_{C-H} aliphatic), 2235, 2195, 2135 cm^{-1} ($\nu_{C=N}$); MS (ESI$^+$) calcd: *m*/*z*: 145.1 ($[C_8H_{17}S]^+$); found: *m*/*z*: 145.1047.

[S1]NO$_3$: White solid, yield: 92%; MW, 165.05. ^{1}H NMR (DMSO, 500 MHz): δ=3.43 (m, 2H), 3.24 (m, 2H), 2.73 (s, 3H), 2.20 (m, 2H), 2.09 ppm (m, 2H); IR: $\tilde{\nu}$=2983, 2948 (ν_{C-H} aliphatic), 2395, 1762, 1382 cm^{-1} (ν_{NO_3}); MS (ESI$^+$) calcd: *m*/*z*: 103.06 ($[C_5H_{11}S]^+$); found: *m*/*z*: 103.0579.

[S2]NO$_3$: Colorless liquid, yield: 94%; MW, 179.06. ^{1}H NMR (DMSO, 500 MHz): δ=3.44 (m, 2H), 3.35 (m, 2H), 3.16 (m, 2H), 2.16 (m, 2H), 2.10 (m, 2H), 1.29 ppm (t, 3H); IR: $\tilde{\nu}$=2977, 2948, 2881 (ν_{C-H} aliphatic), 2394, 1762, 1349 cm^{-1} (ν_{NO_3}); MS (ESI$^+$) calcd: *m*/*z*: 117.07 ($[C_6H_{13}S]^+$); found: *m*/*z*: 117.0734.

[S4]NO$_3$: White solid, yield: 89%; MW, 207.09. ^{1}H NMR (DMSO, 500 MHz): δ=3.46 (m, 2H), 3.34 (m, 2H), 3.15 (m, 2H), 2.18 (m, 2H), 2.12 (m, 2H), 1.64 (m, 2H), 1.37 (m, 2H), 0.89 ppm (t, 3H); IR: $\tilde{\nu}$=2960, 2940, 2874 (ν_{C-H} aliphatic), 2396, 1762, 1377 cm^{-1} (ν_{NO_3}); MS (ESI$^+$) calcd: *m*/*z*: 145.1 ($[C_8H_{17}S]^+$); found: *m*/*z*: 145.1047.

[S1]Sac: Colorless viscous liquid, yield: 91%; MW, 285.05. ^{1}H NMR (CD_3COCD_3, 500 MHz): δ=7.64 (m, 4H), 3.82 (m, 2H), 3.60 (m, 2H), 3.07 (s, 3H), 1.93 (m, 2H), 1.73 ppm (m, 2H); IR: $\tilde{\nu}$=2942, 2870, 1460 (ν_{C-H} aliphatic), 1333 (ν_{CNS}), 1258, 1145 (ν_{SO_2}), 950 cm^{-1} (ν_{CNS}); MS (ESI$^+$) calcd: *m*/*z*: 103.06 ($[C_5H_{11}S]^+$).

[S2]Sac: Colorless viscous liquid, yield: 92%; MW, 299.06. ^{1}H NMR (CD_3COCD_3, 500 MHz): δ=7.63 (m, 4H), 3.81 (m, 2H), 3.68 (m, 2H), 3.52 (m, 2H), 2.42 (m, 2H), 2.35 (m, 2H), 1.47 ppm (t, 3H); IR: $\tilde{\nu}$=2944, 2875, 1455, 1417, 1386 (ν_{C-H} aliphatic), 1329 (ν_{CNS}), 1257, 1145 (ν_{SO_2}), 949 cm^{-1} (ν_{CNS}); MS (ESI$^+$) calcd: *m*/*z*: 117.07 ($[C_6H_{13}S]^+$); found: *m*/*z*: 117.0734.

[S4]Sac: Colorless viscous liquid, yield: 87%; MW, 327.10. ^{1}H NMR (DMSO, 500 MHz): δ=7.63 (m, 4H), 3.54 (m, 2H), 2.58 (m, 2H), 3.32 (m, 2H), 1.84 (m, 2H), 1.80 (m, 2H), 1.55 (m, 2H), 1.50 (m, 2H), 1.38 ppm (t, 3H); IR: $\tilde{\nu}$=2959, 2934, 2873, 1455 (ν_{C-H} aliphatic), 1329 (ν_{CNS}), 1256, 1145 (ν_{SO_2}), 949 cm^{-1} (ν_{CNS}); MS (ESI$^+$) calcd: *m*/*z*: 145.1 ($[C_8H_{17}S]^+$); found: *m*/*z*: 145.1047.

Acknowledgements

This work was supported by the National Natural Science Foundation of China (No. 20533080, 20225309, and 50421502). We are grateful to Ms. Ling Gao and Mr. Qixiu Zhu for their assistance with this work.

[1] a) T. Welton, *Chem. Rev.* **1999**, *99*, 2071–2083; b) J. C. B. Richard, J. D. Paul, J. E. David, W. Thomas, *Chem. Commun.* **2001**, 1862–1863; c) E. Kuhlmann, S. Himmler, H. Giebelhaus, P. Wasserscheid, *Green Chem.* **2007**, *9*, 233–242.

[2] a) C. Ye, J. M. Shreeve, *J. Org. Chem.* **2004**, *69*, 6511–6513; b) Y. Fukaya, Y. Iizuka, K. Sekikawa, H. Ohno, *Green Chem.* **2007**, *9*, 1155–1157.

[3] a) A. J. Boydston, C. S. Pecinovsky, S. T. Chao, C. W. Bielawski, *J. Am. Chem. Soc.* **2007**, *129*, 14550–14551; b) K. Fukumoto, M. Yoshizawa, H. Ohno, *J. Am. Chem. Soc.* **2005**, *127*, 2398–2399.

[4] a) H. Ohno, *Electrochemical Aspects of Ionic Liquids*, Wiley, New Jersey, **2005**; b) B. O'Regan, M. Grätzel, *Nature* **1991**, *353*, 737–740.

[5] P. Wasserscheid, T. Welton, *Ionic Liquids in Synthesis*, VCH, Weinheim, **2003**.

[6] a) P. Wasserscheid, W. Keim, *Angew. Chem.* **2000**, *112*, 3926–3945; *Angew. Chem. Int. Ed.* **2000**, *39*, 3772–3789; b) T. J. Geldbach, P. J. Dyson, *J. Am. Chem. Soc.* **2004**, *126*, 8114–8115.

[7] a) C. Ye, W. Liu, Y. Chen, L. Yu, *Chem. Commun.* **2001**, 2244–2245; b) Y. Wang, H. Yang, *J. Am. Chem. Soc.* **2005**, *127*, 5316–5317; c) K. Ding, Z. Miao, Z. Liu, Z. Zhang, B. Han, G. An, S. Miao, Y. Xie, *J. Am. Chem. Soc.* **2007**, *129*, 6362–6363.

[8] a) J. G. Huddlestou, H. D. Willauer, R. P. Swatloski, A. E. Visser, R. D. Rogers, *Chem. Commun.* **1998**, 1765–1766; b) A. Bösmann, L. Datsevich, A. Jess, A. Lauter, C. Schmitz, P. Wasserscheid, *Chem. Commun.* **2001**, 2494–2495.

[9] a) R. M. Lau, F. Rantwijk, K. R. Seddon, R. A. Sheldon, *Org. Lett.* **2000**, *2*, 4189–4191; b) J. L. Kaar, A. M. Jesionowski, J. A. Berberich, R. Moulton, A. J. Russell, *J. Am. Chem. Soc.* **2003**, *125*, 4125–4131.

[10] a) J. S. Wilkes, M. J. Zaworotko, *J. Chem. Soc. Chem. Commun.* **1992**, 965–967; b) P. Bonhôte, A. P. Dias, N. Papageorgiou, K. Kalyanasundaram, M. Grätzel, *Inorg. Chem.* **1996**, ***35***, 1168–1178.

[11] a) J. Sun, D. R. MacFarlane, M. Forsyth, *Electrochim. Acta* **2003**, *48*, 1707–1711; b) J. Golding, N. Hamid, D. R. MacFarlane, M. Forsyth, C. Forsyth, C. Collins, J. Huang, *Chem. Mater.* **2001**, *13*, 558–564.

[12] a) Z. B. Zhou, H. Matsumoto, K. Tatsumi, *Chem. Eur. J.* **2005**, *11*, 752–766; b) J. Pernak, A. Syguda, I. Mirska, A. Pernak, J. Nawrot, A. Pradzyñska, S. T. Griffin, R. D. Rogers, *Chem. Eur. J.* **2007**, *13*, 6817–6827.

[13] a) R. P. Singh, J. M. Shreeve, *Inorg. Chem.* **2003**, *42*, 7416–7421; b) J. Zhang, G. R. Martin, D. D. DesMarteau, *Chem. Commun.* **2003**, 2334–2335.

[14] a) N. M. M. Mateus, L. C. Branco, N. M. T. Lourenço, C. A. M. Afonso, *Green Chem.* **2003**, *5*, 347–352; b) L. Yu, D. Garcia, R. Ren, X. Zeng, *Chem. Commun.* **2005**, 2277–2279.

[15] See: *Proceedings of the Second International Congress on Ionic Liquids*, Yokohama, Japan, August, 5–7, 2007.

[16] a) B. Garcia, S. Lavallée, G. Perron, C. Michot, M. Armand, *Electrochim. Acta* **2004**, *49*, 4583–4588; b) H. Sakaebe, H. Matsumoto, *Electrochem. Commun.* **2003**, *5*, 594–598.

[17] a) M. A. B. H. Susan, A. Noda, S. Mitsushima, M. Watanabe, *Chem. Commun.* **2003**, 938–939; b) R. F. Souza, J. C. Padilha, R. S. Goncalves, J. Dupont, *Electrochem. Commun.* **2003**, *5*, 728–731.

[18] a) M. Ue, M. Takeda, A. Toriumi, A. Kominato, R. Hagiwara, Y. Ito, *J. Electrochem. Soc.* **2003**, *150*, 499–502; b) Y. J. Kim, Y. Matsuzawa, S. Ozaki, K. C. Park, C. Kim, M. Endo, H. Yoshida, G. Masuda, T. Sato, M. S. Dresselhausc, *J. Electrochem. Soc.* **2005**, *152*, 710–715.

[19] a) N. Papageorgiou, Y. Athanassov, M. Armand, P. Bonh ote, H. Pettersson, A. Azam, M. Gïratzel, *J. Electrochem. Soc.* **1996**, *143*, 3099–3108; b) P. Wang, S. M. Zakeeruddin, J.-E. Moser, R. Humphry-Baker, M. Grätzel, *J. Am. Chem. Soc.* **2004**, *126*, 7164–7165.

[20] Z. Fei, T. J. Geldbach, D. Zhao, P. J. Dyson, *Chem. Eur. J.* **2006**, *12*, 2122–2130.

[21] E. D. Bates, R. D. Mayton, I. Ntai, J. H. Davis, Jr., *J. Am. Chem. Soc.* **2002**, *124*, 926–927.

[22] H. Itoh, K. Naka, Y. Chujo, *J. Am. Chem. Soc.* **2004**, *126*, 3026–3027.

[23] W. Miao, T. H. Chan, *J. Org. Chem.* **2005**, *70*, 3251–3255.

[24] Z. Fei, D. Zhao, T. J. Geldbach, R. Scopelliti, P. J. Dyson, *Chem. Eur. J.* **2004**, *10*, 4886–4893.

[25] D. Zhao, Z. Fei, T. J. Geldbach, R. Scopelliti, P. J. Dyson, *J. Am. Chem. Soc.* **2004**, *126*, 15876–15882.

[26] A. E. Visser, R. P. Swatloski, W. M. Reichert, R. Mayton, S. Sheff, A. Wierzbicki, J. H. Davis, Jr., R. D. Rogers, *Chem. Commun.* **2001**, 135–136.

[27] a) D. R. MacFarlane, J. Golding, S. Forsyth, M. Forsyth, G. B. Deacon, *Chem. Commun.* **2001**, 1430–1431; b) M. Yoshizawa, H. Ohno, *Chem. Commun.* **2004**, 1828–1829.

[28] M. Yoshizawa, W. Xu, C. A. Angell, *J. Am. Chem. Soc.* **2003**, *125*, 15411–15419.
[29] J. N. Barisci, G. G. Wallace, D. R. MacFarlane, R. H. Baughman, *Electrochem. Commun.* **2004**, *6*, 22–27.
[30] H. Matsumoto, H. Sakaebe, K. Tatsumi, *J. Power Sources* **2005**, *146*, 45–50.
[31] O. O. Okoturo, T. J. VanderNoot, *J. Electroanal. Chem.* **2004**, *568*, 167–181.
[32] H. Matsumoto, T. Matsuda, Y. Miyazaki, *Chem. Lett.* **2000**, 1430–1431.
[33] D. Gerhard, S. C. Alpaslan, H. J. Gores, M. Uerdingen, P. Wasserscheid, *Chem. Commun.* **2005**, 5080–5081.
[34] a) L. Yang, Z. X. Zhang, X. H. Gao, H. Q. Zhang, K. Mashita, *J. Power Sources* **2006**, *162*, 614–619; b) S. Fang, L. Yang, C. Wei, C. Peng, K. Tachibana, K. Kamijima, *Electrochem. Commun.* **2007**, *9*, 2696–2702; c) H. Paulsson, A. Hagfeldt, L. Kloo, *J. Phys. Chem. B* **2003**, *107*, 13665–13670.
[35] a) P. Wang, F. Gao, Y. Cao, J. Zhang, Chinese Patent, CN 200710055896.3; b) C. Xi, Y. Cao, Y. Cheng, M. Wang, X. Jing, S. M. Zakeeruddin, M. Grätzel, P. Wang, *J. Phys. Chem. C* **2008**, *112*, 11063–11067.
[36] a) H. Shirota, E. W. Castner, Jr., *J. Phys. Chem. B* **2005**, *109*, 21576–21585; b) D. Zhao, *Aust. J. Chem.* **2004**, *57*, 509; c) J. Wang, H. Wang, S. Zhang, H. Zhang, Y. Zhao, *J. Phys. Chem. B* **2007**, *111*, 6181–6188.
[37] a) B. A. DaSilveira, Neto, L. S. Santos, F. M. Nachtigall, M. N. Eberlin, J. Dupont, *Angew. Chem.* **2006**, *118*, 7409–7412; *Angew. Chem. Int. Ed.* **2006**, *45*, 7251–7254; b) B. A. DaSilveira, Neto, L. S. Santos, F. M. Nachtigall, M. N. Eberlin, J. Dupont, *Angew. Chem.* **2006**, *118*, 1–1; *Angew. Chem. Int. Ed.* **2006**, *45*, 1–5.
[38] H. Chen, Z. Ouyang, R. G. Cooks, *Angew. Chem.* **2006**, *118*, 3738–3742; *Angew. Chem. Int. Ed.* **2006**, *45*, 3656–3660.
[39] a) F. C. Gozzo, L. S. Santos, R. Augusti, C. S. Consorti, J. Dupont, M. N. Eberlin, *Chem. Eur. J.* **2004**, *10*, 6187–6193; b) B. K. Ku, J. F. de. la. Mora, *J. Phys. Chem. B* **2004**, *108*, 14915–14923; c) R. Bini, O. Bortolini, C. Chiappe, D. Pieraccini, T. Siciliano, *J. Phys. Chem. B* **2007**, *111*, 598–604; d) J. W. Remsburg, R. J. Soukup-Hein, J. A. Crank, Z. S. Breitbach, T. Payagala, D. W. Armstrong, *J. Am. Soc. Mass Spectrom.* **2008**, *19*, 261–269.
[40] a) E. F. Smith, I. J. V. Garcia, D. Briggs, P. Licence, *Chem. Commun.* **2005**, 5633–5635; b) D. S. Silvester, T. L. Broder, L. Aldous, C. Hardacre, A. Crossley, R. G. Compton, *Analyst* **2007**, *132*, 196–198; c) F. Maier, J. M. Gottfried, J. Rossa, D. Gerhard, P. S. Schulz, W. Schwieger, P. Wasserscheid, H.-P. Steinrück, *Angew. Chem.* **2006**, *118*, 7778–7780; *Angew. Chem. Int. Ed.* **2006**, *45*, 7942–7944.
[41] S. Caporali, U. Bardi, A. Lavacchi, *J. Electron Spectrosc. Relat. Phenom.* **2006**, *151*, 4–8.
[42] a) O. Höfft, S. Bahr, M. Himmerlich, S. Krischok, J. A. Schaefer, V. Kempter, *Langmuir* **2006**, *22*, 7120–7123; b) V. Lockett, R. Sedev, C. Bassell, J. Ralston, *Phys. Chem. Chem. Phys.* **2008**, *10*, 1330–1335.
[43] M. Gottfried, F. Maier, J. Rossa, D. Gerhard, P. S. Schulz, P. Wasserscheid, H.-P. Steinrück, *Z. Phys. Chem.* **2006**, *220*, 1439–1453.
[44] E. F. Smith, F. J. M. Rutten, I. J. Villar-Garcia, D. Briggs, P. Licence, *Langmuir*, **2006**, *22*, 9386–9392.
[45] a) D. R. MacFarlane, J. Huang, M. Forsyth, *Nature*, **1999**, *402*, 792–794; b) C. M. Forsyth, D. R. MacFarlane, J. J. Golding, J. Huang, J. Sun, M. Forsyth, *Chem. Mater.* **2002**, *14*, 2103–2108.
[46] a) J. C. Dearden, *Sci. Total Environ.* **1991**, *109–110*, 59–68; b) R. J. C. Brown, R. F. C. Brown, *J. Chem. Educ.* **2000**, *77*, 724–731.
[47] D. R. MacFarlane, S. A. Forsyth, J. Golding, G. B. Deacon, *Green Chem.* **2002**, *4*, 444–448.
[48] O. O. Okoturo, T. J. VanderNoot, *J. Electroanal. Chem.* **2004**, *568*, 167–181.
[49] Q. Zhang, Z. Li, J. Zhang, S. Zhang, L. Zhu, J. Yang, X. Zhang, Y. Deng, *J. Phys. Chem. B* **2007**, *111*, 2864–2872.
[50] J. Fuller, R. Carlin, R. Osteryoung, *J. Electrochem. Soc.* **1997**, *144*, 3881–3885.

Received: April 2, 2008
Revised: August 14, 2008
Published online: November 28, 2008

